Mechanics of Advanced Materials and Structures

ISSN: (Print) (Online) Journal homepage: https://www.tandfonline.com/loi/umcm20

On the splay deformation mode of a polar linearly elastic bar stretched by its own weight

K. P. Soldatos

To cite this article: K. P. Soldatos (09 Feb 2024): On the splay deformation mode of a polar linearly elastic bar stretched by its own weight, Mechanics of Advanced Materials and Structures, DOI: 10.1080/15376494.2024.2313151

To link to this article: https://doi.org/10.1080/15376494.2024.2313151

Published online: 09 Feb 2024.

MECHANICS OF ADVANCED MATERIALS AND STRUCTURES
https://doi.org/10.1080/15376494.2024.2313151

Taylor & Francis
Taylor & Francis Group

ORIGINAL ARTICLE

OPEN ACCESS Check for updates

On the splay deformation mode of a polar linearly elastic bar stretched by its own weight

K. P. Soldatos

School of Mathematical Sciences, University of Nottingham, Nottingham, UK

ABSTRACT

This communication considers the fundamental linear elasticity problem of a prismatic bar, or plate, stretched by its own weight and examines the impact of its classical solution in the regime of isotropic and anisotropic polar material elasticity. Accordingly, the existing non-polar elasticity solution of such a self-stretched isotropic bar is initially extended to embrace appropriate classes of non-polar material anisotropy. This extension verifies that, in non-polar transverse isotropy and special orthotropy, the attained solution is exclusively dominated by splay-type features of deformation. Attention then focuses on the influence that the observed fiber-splay deformation mode, as well as its fiber-bending deformation counterpart, exert on the formulation and potential solution of corresponding boundary value problems met in polar linear elasticity. It is seen that, regardless of the isotropic or anisotropic material symmetries considered, the outlined process may lead to solution of relevant boundary value problems that are slightly different to their non-polar elasticity counterparts. This conclusion reinforces the role that a polar material version of the theorem of minimum potential energy, and relevant energy minimization approaches, can play in the search for full solution of boundary value problems met polar material elasticity.

ARTICLE HISTORY
Received 17 January 2024
Accepted 29 January 2024

KEYWORDS
Anisotropic elasticity; Cosserat theory; couple-stress theory; elasticity; fibre-reinforced plates; fibres with bending stiffness; polar materials; polar linear elasticity; self-stretched bar

1. Introduction

While several aspects of the theory of solids reinforced with fibers possessing bending stiffness [1, 2] are still developing (see also [3]), it is already understood (e.g. [4–8]) that, in general, there exist three principal deformation modes observable during the deformation of a relevant fibrous composite. These have become known as the fiber-bending, the fiber-splay, and the fiber-twist deformation modes, they are generally (though not necessarily) coupled, and they all contribute to couple-stress generation (or accumulation). The fiber-bending mode has generally been considered more influential than either of its other two counterparts, and the theory [1, 2] thus has become more generally known as the theory of materials reinforced with fibers resistant in bending (or possessing bending stiffness).

Moreover, there have also become available two simpler, restricted versions of the full theory. One of these is specialized to predominantly capture effects that are due to fiber-bending, while the other to capture effects due to fiber-splay deformations. Either of those simpler versions of the unrestricted (full) theory makes use of a reduced number of fiber-stiffness elastic moduli. This attractive feature facilitates their use in more practical and computational applications (e.g. [9–14]) and, also, encourages efforts that improve understanding of their relationship/relevance with the full theory [1, 2]. Such efforts are naturally benefited from use of engineering intuition and are greatly assisted from comparisons of relevant analytical or computational results stemming from the solution of simple or more advanced structural analysis boundary value problems.

In this context, the classical linear elasticity problem of the pure bending of a rectangular plate (or prismatic bar) has already been employed to this effect. Its classical, elementary solution, available in conventional (non-polar) isotropic linear elasticity (e.g. [15], Ch. 9), is long ago extended in Koiter's pioneering effort [16] to exemplify and demonstrate principal features that are dominant in linearly isotropic couple-stress elasticity.

Due to its simplicity, that bending problem [15, 16] admits an exact, closed form solution underpinned by displacements that are quadratic in the co-ordinate parameters. Displacement gradients and, therefore, strains, rotations, and non-zero stresses thus are all linear in the same. Consequently, all non-zero curvature-strains and deviatoric couple-stresses observed in polar linear elasticity are constant throughout the body of the polar elastic plate of interest. Most importantly, and conveniently, further extension of the implied closed form solution, into the regime of linearly anisotropic couple-stress theory [2, 5, 8], leaves unaffected those relatively simple mathematical features of the observed displacement, stress, and couple-stress fields.

CONTACT K. P. Soldatos kostas.soldatos@nottingham.ac.uk School of Mathematical Sciences, University of Nottingham, University Park, Nottingham, NG7 2RD, U.K.

It has accordingly been seen [8] that, in dealing with the pure bending problem of a polar fiber-reinforced plate, the fiber-splay mode/version of the theory fails to provide any kind of reliable information, because this specific boundary value problem is not adequately influenced by fiber-splay deformation features. For the same reason, and by essentially recognizing that neither fiber-twist features are present in that case, the restricted fiber-bending version of the theory provides information that is almost identical to that obtained through use of the full theory.

Motivated by these observations, the present communication emerges through an interest to look at the other end of implied spectrum of boundary value problem applications and, more specifically, to examine the extent to which the outlined conclusions are reversed when all three versions of the theory are employed in modeling problems that are principally influenced by fiber-splay deformation effects. This interest arises from the feeling that, if those conclusions are indeed reversed in that case, then, the version of the theory that might most conveniently fit modeling and study of any relevant boundary value problem could be chosen through intuitive judgment of the place that the considered problem attains within that spectrum.

The problem of a polar, linearly elastic plate stretched by its own weight thus becomes the principal subject of this communication, as its deformation features resemble closely the splay-type characteristics of present interest. The non-polar isotropic material version of this problem is also classical in conventional linear elasticity and falls into the same category with the afore mentioned pure bending problem (see [15], Ch. 9). Its solution is also underpinned by displacements that are quadratic in the co-ordinate parameters and, thus, possesses mathematical properties and features analogous to those involved in its pure bending counterpart.

However, a special feature that makes the study of this problem physically, rather than mathematically different stems from the fact that the deformation pattern of the purely bent polar plate is considered identical to that of its non-polar counterpart and, therefore, known. In contrast, as will be seen and discussed in what follows, the deformation pattern of a self-stretched polar material bar, necessarily though not unexpectedly, differs from that of its non-polar material counterpart.

Under these considerations, Section 2 initially extends the formulation as well as the closed form solution of the non-polar self-stretched isotropic bar problem [15] into the anisotropic non-polar material regime. In doing so, Section 2 considers that the implied non-polar material anisotropy is as advanced as the kind of special orthotropy attained when one of the orthotropy axes is aligned with the gravity direction. The obtained solution thus verifies that the observed deformation pattern is exclusively dominated by fiber-splay deformation effects.

Sections 3 and 4 next consider the special case of transverse isotropy that is due to presence of straight fibers aligned along the gravity direction and possessing bending stiffness, and respectively examine the influence that the obtained non-polar elasticity solution exerts in the afore mentioned unrestricted and restricted versions of polar linear elasticity. The expectation thus is confirmed that the information provided by the restricted fiber-splay version is almost identical to that obtained through use of the full theory, while the other, fiber-bending restricted version fails to offer any kind of reliable relevant information. This stage of the study makes it also clear that the deformation pattern of an anisotropic polar material bar stretched by its own weight differs from its non-polar material counterpart and, thus, essentially remains unknown. Section 5 then shows that, naturally, the same is also true in the case of a self-stretched linearly elastic isotropic bar where, however, the absence of fibers implies that polar material response is an intrinsic material feature of unspecified origin and source.

While the afore mentioned principal question that motivates this study receives a positive answer, the specific boundary value problem of a linearly elastic polar material bar or plate stretched by its own weight remains still open to further investigation. In this context, Section 6 concludes the present part of this investigation by outlining a manner that complete solution of this, as well as other relevant boundary value problems met in couple-stress linear elasticity can be pursued. Namely, by appropriately using the polar material version of the theorem of minimum potential energy [6].

2. Orthotropic, non-polar, prismatic bar stretched by its own weight

Figure 1 resembles closely its counterpart labeled as Figure 143 on page 279 of Ref [15]. Accordingly, in the Cartesian co-ordinate system, $Ox_\alpha x_3$, where Greek indices take the values 1 and 2, the figure illustrates the undeformed configuration (solid lines) and the small deformation pattern (dashed lines) of either of the $x_\alpha x_3$-cross-sections of a

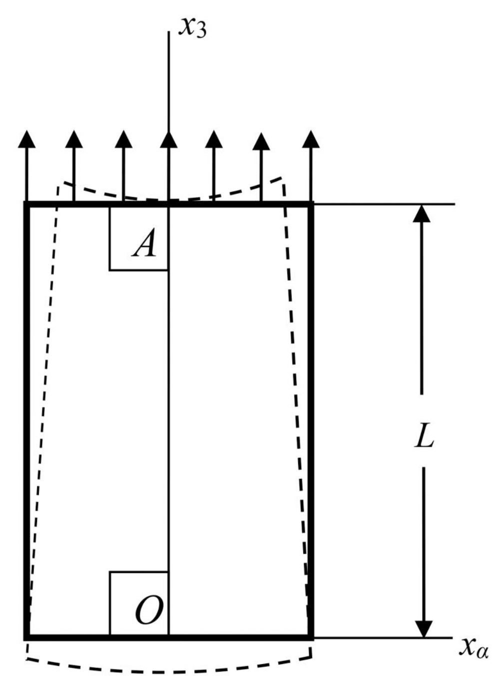

Figure 1. Schematic representation of the undeformed (heavy solid line) and deformed (dashed line) configurations of either of the $x_\alpha x_3$-cross-sections of a prismatic, non-polar, linearly elastic isotropic bar stretched by its own weight [15] ($|x_\alpha| \leq L_\alpha$, $0 \leq x_3 \leq L$).

prismatic, non-polar, linearly elastic isotropic bar (or plate) that is stretched by its own weight. That, essentially self-stretched bar has dimensions $|x_\alpha| \leq L_\alpha$ and $0 \leq x_3 \leq L$. Either cross-section thus passes through the Ox_3-axis of the co-ordinate system and is considered fixed at the middle-point, A, of its top boundary.

If ρ and g denote the material density of the bar and the acceleration of gravity, respectively, the body force, $\mathbf{F}$, that represents the weight per unit volume of the bar has components,

$$F_1 = F_2 = 0, \;\; F_3 = -\rho g. \tag{1}$$

Since the bar is deformed solely by the action of its own weight, it is anticipated that no tractions are applied externally on its lateral and bottom boundaries and that it is in equilibrium under the influence of the following stress field:

$$\sigma_{11} = \sigma_{(12)} = \sigma_{(13)} = \sigma_{22} = \sigma_{(23)} = 0, \;\; \sigma_{33} = \rho g x_3, \tag{2}$$

where enclosure of indices within parentheses implies that the stress tensor is symmetric.

This stress field implies that

$$\sigma_{33}|_{x_3=0} = 0, \;\; \sigma_{33}|_{x_3=L} = \rho g L, \tag{3}$$

and, hence, regardless of the type of the linearly elastic material constitution of the bar, the tensile stress field (2) satisfies exactly (i) all implied zero-stress boundary conditions, and (ii) all three equilibrium equations,

$$\sigma_{(j\alpha),j} = 0, \;\; \sigma_{(j3),j} + F_3 = 0, \tag{4}$$

where, Latin indices take the values 1, 2 and 3, repeated indices indicate summation over their range and, in the usual manner, a comma among indices indicates partial differentiation.

For the purposes of the present study, it is considered that the linearly elastic material of the bar is specially orthotropic, in the sense that its symmetries are characterized by three mutually orthogonal directions of material preference aligned with the co-ordinate axes Ox_i. In that case, the relevant form attained by the generalized Hooke's law (e.g. [17]) may be expressed either in terms of the elastic stiffness moduli, the "C's",

$$\begin{bmatrix}\sigma_{11}\\ \sigma_{22}\\ \sigma_{33}\end{bmatrix} = \begin{bmatrix} C_{11} & C_{12} & C_{13}\\ C_{12} & C_{22} & C_{23}\\ C_{13} & C_{23} & C_{33}\end{bmatrix}\begin{bmatrix}e_{11}\\ e_{22}\\ e_{33}\end{bmatrix}, \begin{pmatrix}\sigma_{(23)}\\ \sigma_{(13)}\\ \sigma_{(12)}\end{pmatrix} = 2\begin{pmatrix}C_{44}e_{23}\\ C_{55}e_{13}\\ C_{66}e_{12}\end{pmatrix}, \tag{5}$$

or, after inversion,

$$\begin{bmatrix}e_{11}\\ e_{22}\\ e_{33}\end{bmatrix} = \begin{bmatrix} S_{11}S_{12}S_{13}\\ S_{12}S_{22}S_{23}\\ S_{13}S_{23}S_{33}\end{bmatrix}\begin{bmatrix}\sigma_{11}\\ \sigma_{22}\\ \sigma_{33}\end{bmatrix}, \;\; \begin{pmatrix}2e_{23}\\ 2e_{13}\\ 2e_{12}\end{pmatrix} = \begin{pmatrix}S_{44}\sigma_{(23)}\\ S_{55}\sigma_{(13)}\\ S_{66}\sigma_{(12)}\end{pmatrix}, \tag{6}$$

in terms of the corresponding elastic compliances, the "S's".

Here, as well as in what follows, use is made of the standard definitions:

$$e_{ij} = \frac{1}{2}(u_{i,j} + u_{j,i}), \qquad \omega_{ij} = \frac{1}{2}(u_{i,j} - u_{j,i}), \tag{7}$$

of the small strain and rotation tensors, which essentially emerge as the symmetric and the antisymmetric part, respectively, of the displacement gradient tensor $u_{i,j}$.

Introduction of the stress field (2) into (6) makes immediately understood the splay-type nature of the shelf-stretched bar deformation. This is characterized by the fact that only the three normal components of the strain field are nonzero. Further use of the definition (7a) of the strain tensor leads to the following set of six simultaneous partial differential equations (PDEs) for the three unknown displacement components:

$$\begin{pmatrix}u_{1,1}\\ u_{2,2}\\ u_{3,3}\end{pmatrix} = \begin{pmatrix}S_{13}\\ S_{23}\\ S_{33}\end{pmatrix}\rho g x_3, \;\; u_{1,2} + u_{2,1} = u_{1,3} + u_{3,1} = u_{2,3} + u_{3,2} = 0. \tag{8}$$

The integration procedure of this set of PDEs resembles its counterpart detailed in [15] for the corresponding linearly elastic isotropic bar. It, thus, requires elimination of interfering rigid body rotations and a relevant rigid body translation. This elimination is enabled with implementation of the afore mentioned displacement condition,

$$u_i\Big|_{\substack{x_\alpha = 0\\ x_3 = L}} = 0, \tag{9}$$

and leads to the displacement field:

$$u_1 = \rho g S_{13} x_1 x_3, \;\; u_2 = \rho g S_{23} x_2 x_3,$$
$$u_3 = \frac{1}{2}\rho g\left[S_{33}\left(x_3^2 - L^2\right) - \left(S_{13}x_1^2 + S_{23}x_2^2\right)\right]. \tag{10}$$

Equations (2), (6) and (10) thus represent the exact closed form solution of the self-stretched orthotropic bar problem. It can readily be verified that in the special case of a corresponding linearly elastic isotropic bar, where the appearing compliance moduli relate to the Young's modulus and the Poisson's ratio a follows:

$$S_{33} = 1/E, \;\; S_{13} = S_{23} = -\nu/E, \tag{11}$$

the obtained solution reduces to its counterpart [15] that is schematically represented in Figure 1.

In the present study, Figure 1 still provides adequate qualitative information regarding the deformation pattern attained by the implied orthotropic bar. However, precise geometrical features of the appearing dashed lines are naturally regulated by the variety of the actual numerical values that the elastic compliance moduli, S_{13}, S_{23} and S_{33}, can be associated with a material that characterized by the implied symmetries of special orthotropy.

The remaining of this investigation is adequately bounded by symmetries of material orthotropy that is due to presence of two orthogonal families of straight fibers. One of those families is parallel to the gravity direction, Ox_3, while the other may be selected parallel to either of the horizontal co-ordinate axes, Ox_α.

A couple of simpler special cases further arise by considering that only one of the implied pair of fiber families is present. The resulting fibrous composite then acquires the simpler anisotropy features of a transversely isotropic material. While the mathematical description and outlined solution of the problem thus simplifies, the implied simplification leaves largely unaffected the qualitative solution features as well as the principal physical observations.

In this regard, it is adequate for the purposes of present study to later consider, for more detailed investigation, only one of the implied cases of transverse isotropy. Namely, the pilot study (see Section 3.2 onwards) in which the anticipated single family of straight fibers is parallel to the gravity direction, Ox_3. In that case, the following additional relationships accompany the elastic moduli appearing in (5):

$$C_{11} = C_{22},\ C_{13} = C_{23},\ C_{44} = C_{55},\ C_{66} = \frac{1}{2}(C_{22} - C_{12}), \tag{12}$$

and subsequently influence the compliance moduli appearing in (6) through similar connections,

$$S_{11} = S_{22},\ S_{13} = S_{23},\ S_{44} = S_{55} = 1/C_{44},\ S_{66} = 1/C_{66} = 2/(C_{22} - C_{12}). \tag{13}$$

Provided that (i) the fibers are perfectly flexible, in the sense that they do not resist but just follow the bulk deformation of the transverse isotropic composite, and (ii) the implied fibrous composite does not exhibit inherent properties of polar material behavior, the outlined solution is complete and, thus, needs no further mathematical consideration or treatment.

3. Effect of polar material behavior due to fiber bending stiffness – unrestricted theory

As is already mentioned, deformation patterns of polar fibrous composites when fibers possess bending stiffness are generally composed by three principal deformation modes. These became known as fiber-bending, fiber-splay, the fiber-twist deformation modes (see Section 9 of [1]). They all contribute to couple-stress generation and are generally coupled. In the case of the unrestricted linearized version of the theory [1, 2], which is the subject of this investigation, that coupling is manifested in the form of the polar part of the strain energy function, though, as will be verified in what follows, its strength also depends on the kind of the deformation that the elastic solid is subjected to.

3.1. Preliminary concepts and equilibrium equations

Under these considerations, it is recalled (e.g. [1–3]) that the strain energy function of any linearly elastic fibrous composite with fiber bending stiffness is of the form:

$$W = W^e(\mathbf{e}) + W^k(\boldsymbol{\kappa}) \geq 0, \tag{14}$$

where W^e is the quadratic, positive definite strain energy function that describes the response of the corresponding non-polar solid, and W^k is its polar material counterpart that is positive semi-definite and quadratic in the components of a tensor, $\boldsymbol{\kappa}$, that captures curvature-type features of fiber deformation.

In dealing with the classes of fibrous composites considered in the preceding section, the well-known quadratic form of W^e anticipates validity of the following relationships:

$$W^e(\mathbf{e}) = \frac{1}{2}\sigma_{(ij)}e_{ji},\ \ \sigma_{(ij)} = \frac{\partial W^e}{\partial e_{ij}}, \tag{15}$$

the second of which leads to linear constitutive equations of the form (5).

On the other hand, the components of the deviatoric couple-stress tensor, $\bar{\mathbf{m}}$, and the curvature tensor, $\boldsymbol{\kappa}$, relate with the polar part, W^k, of the strain energy function (14) through expressions analogous to (15). However, as will be seen in what follows, the precise form of those expressions depends on the form that $\boldsymbol{\kappa}$ attains in each of the afore mentioned versions of the polar elasticity theory of interest (e.g. [1, 4, 7]).

It is meanwhile recalled that the assumed polar material behavior requires replacement of the equilibrium equations (4) with their polar material counterparts,

$$\sigma_{(ij),i} + \frac{1}{2}\varepsilon_{kji}\bar{m}_{\ell k,\ell i} + \delta_{j3}F_3 = 0, \quad \sigma_{[ij]} = \frac{1}{2}\varepsilon_{kji}m_{\ell k,\ell}, \tag{16}$$

where $\mathbf{m}$ represents the couple-stress tensor and

$$\bar{m}_{\ell k} = m_{\ell k} - \frac{1}{3}m_{rr}\delta_{\ell k}, \tag{17}$$

are the components of its deviatoric part. In this context, (16b) is regarded as a constitutive equation that provides the antisymmetric part of the stress in terms of the couple-stress gradients, thus leaving (16a) as the only, appropriately augmented version of an equilibrium equation.

A final set of equations that also need to be employed, for evaluation of the appearing spherical part of the couple-stress m_{rr}, is described as follows [2, 3, 18]:

$$\Omega_\ell m_{rr,\ell} = 6W^m - 3(\bar{m}_{\ell i}\Omega_i)_{,\ell},\ \ \Omega_i = \frac{1}{2}\varepsilon_{ijk}\omega_{kj} = \frac{1}{2}\varepsilon_{ijk}u_{k,j},\ \ \Omega_{i,i} = 0, \tag{18}$$

where the scalar term W^m appearing in (18a) will be determined as an appropriate part of the form attained by the polar part, W^k, of the strain energy function (14). It is also recalled that the identity (18c) is a consequence of the definitions (18b) and (7b).

It is fitting at this point to mention that, as far as the boundary value problem of present interest is concerned, a combination of (18b) with the displacement field (10) provides the appearing components of the spin vector, $\boldsymbol{\Omega}$, as follows:

$$\Omega_1 = -\rho g S_{13}x_2,\ \ \Omega_2 = \rho g S_{23}x_1 = \rho g S_{13}x_1,\ \ \Omega_3 = 0, \tag{19}$$

where (13b) has also been taken into consideration.

3.2. Polar part of the constitutive equations for the unrestricted version of the theory

In the case that a linearly elastic polar fibrous composite has embedded a single family of straight fibers with bending stiffness, the polar part of the constitutive equations is as follows [4]:

$$\bar{m}_{\ell r} = \frac{2}{3}\varepsilon_{rsi}\left(\frac{\partial W^k}{\partial \kappa_{i\ell}}a_s + \frac{\partial W^k}{\partial \kappa_{is}}a_\ell\right), \quad \bar{m}_{kk} = 0, \tag{20}$$

where the appearing fiber direction vector, **a**, is constant, while, in components, the appearing fiber curvature tensor and its symmetric and antisymmetric counterparts, are

$$\kappa_{ij} = u_{i,kj}a_k, \quad \kappa_{(ij)} = \frac{1}{2}(u_{i,jk} + u_{j,ik})a_k = e_{ij,k}a_k,$$
$$\kappa_{[ij]} = \frac{1}{2}(u_{i,jk} - u_{j,ik})a_k = \omega_{ij,k}a_k. \tag{21}$$

Moreover, the appearing polar part of the strain energy function attains the form

$$W^\kappa = \beta_1(\kappa_{nn})^2 + \beta_2\kappa_{nn}a_k\kappa_{(km)}a_m + \beta_3\kappa_{(km)}\kappa_{(mk)} + \beta_4 a_k\kappa_{(km)}\kappa_{(mn)}a_n + \beta_5\kappa_{[km]}\kappa_{[mk]} + \beta_6 a_k\kappa_{[km]}\kappa_{[mn]}a_n + \beta_7 a_k\kappa_{(km)}\kappa_{[mn]}a_n + \hat{\beta}_3(a_k\kappa_{(km)}a_m)^2, \tag{22}$$

where the coefficients β_1 to β_7, and $\hat{\beta}_3$ represent a set of eight elastic moduli associated with the polar part of the material response. As is shown in [4], positive semi-definiteness of W^κ requires from the values of those elastic moduli to satisfy the following inequalities:

$$\beta_1 \geq 0, \beta_3 \geq 0, \beta_4 \geq 0, \beta_5 \leq 0, \beta_7^2 \leq -4(2\beta_5 + \beta_6)(2\beta_3 + \beta_4),$$
$$\beta_2 + \hat{\beta}_3 \geq 0, \quad \beta_1 + \beta_2 + \beta_3 + \beta_4 + \hat{\beta}_3 \geq \frac{(\beta_1 + \beta_2/2)^2}{\beta_1 + \beta_3/2}. \tag{23}$$

Combination of (20) and (22) then yields the constitutive equation

$$\bar{m}_{\ell r} = \frac{2}{3}\varepsilon_{r\ell s}a_s(2\beta_1\kappa_{nn} + \beta_2\kappa_{km}a_k a_m) + \frac{2}{3}\varepsilon_{ris}a_s\big(2\beta_3\kappa_{(i\ell)} + \beta_4\kappa_{(in)}a_n a_\ell\big) - \frac{1}{3}\varepsilon_{ris}\{4\beta_5(a_s\kappa_{[i\ell]} + a_\ell\kappa_{[is]}) - 2\beta_6 a_n a_\ell(a_i\kappa_{[sn]} - 2a_s\kappa_{[in]}) + \beta_7 a_n a_\ell(a_i\kappa_{ns} - 2a_s\kappa_{in})\}, \tag{24}$$

which evidently receives no contribution from the part

$$W^m = \hat{\beta}_3(a_k\kappa_{(km)}a_m)^2, \tag{25}$$

of the strain energy function (22).

Hence, seven of the eight elastic moduli involved in (22) contribute to the couple-stress constitutive equation (24) and one is associated with the apparently unused part (25) of the stored elastic energy. That part of energy, W^m, is necessarily related with the action of the spherical part of the couple-stress that remains to be determined by solving the PDE that is finally formed by inserting (25) into (18a).

3.3. Effect of polar material behavior on the non-polar elasticity solution of the self-stretched bar

In the present case of principal interest, where the bar depicted in Figure 1 is reinforced with fibers oriented parallel to gravity, it is

$$\mathbf{a} = (0, 0, 1)^T. \tag{26}$$

The constitutive equation (24) thus attains the special form

$$\bar{m}_{\ell r} = \frac{2}{3}\varepsilon_{r\ell 3}(2\beta_1\kappa_{nn} + \beta_2\kappa_{33}) + \frac{2}{3}\varepsilon_{ri3}\big(2\beta_3\kappa_{(i\ell)} + \beta_4\kappa_{(i3)}a_\ell\big) - \frac{2}{3}\varepsilon_{ri3}\big(2\beta_5\kappa_{[i\ell]} - 2\beta_6 a_\ell\kappa_{[i3]} - \beta_7 a_\ell\kappa_{i3}\big) - \frac{1}{3}a_\ell\left[\varepsilon_{r3s}\big(-2\beta_6\kappa_{[s3]} + \beta_7\kappa_{3s}\big) - \frac{4}{3}\beta_5\varepsilon_{ris}\kappa_{[is]}\right], \tag{27}$$

while (25) also simplifies and becomes

$$W^m = \hat{\beta}_3\kappa_{33}^2. \tag{28}$$

On the other hand, a combination of (21) with the displacement field (10) reveals that the non-polar elasticity solution of this boundary value problem associates to (27) only three non-zero curvature components, namely

$$(\kappa_{11}, \kappa_{22}, \kappa_{33}) = \rho g(S_{13}, S_{23}, S_{33}) = \rho g(S_{13}, S_{13}, S_{33}), \tag{29}$$

where (13b) is also accounted for. The constitutive equation (27) then simplifies into the following:

$$\bar{m}_{\ell r} = \frac{2}{3}\varepsilon_{r\ell 3}\left[2\beta_1(\kappa_{11} + \kappa_{22}) + (2\beta_1 + \beta_2)\kappa_{33}\right] + \frac{4}{3}\varepsilon_{r\alpha 3}\beta_3\kappa_{(\alpha\ell)}. \tag{30}$$

and, through use of (29), produces only two non-zero deviatoric couple-stress components,

$$\bar{m}_{12} = -\bar{m}_{21} = -\rho g\lambda, \quad \lambda = \frac{2}{3}\left[2(2\beta_1 + \beta_3)S_{13} + (2\beta_1 + \beta_2)S_{33}\right], \tag{31}$$

which are both constant.

Accordingly, all three normal components of the deviatoric couple-stress are equal to zero ($\bar{m}_{11} = \bar{m}_{22} = \bar{m}_{33} = 0$) and (17) thus yields:

$$m_{11} = m_{22} = m_{33} = \frac{1}{3}m_{rr}. \tag{32}$$

Determination of all three normal couple-stresses then requires solution of the PDE

$$x_1 m_{rr,2} - x_2 m_{rr,1} = 6\rho g\left(\hat{\beta}_3\frac{S_{33}^2}{S_{13}} + \lambda\right) \equiv \tilde{\lambda}, \tag{33}$$

which is obtained by inserting (19), (28) and (31) into (18a).

Use of the method of characteristic lines (see Appendix A) provides the following solution of the PDE (33):

$$\begin{aligned} &x_1^2 + x_2^2 = c_1^2, \\ &m_{rr}(x_1, x_2(x_1), x_3) = \mp\tilde{\lambda}\sin^{-1}(x_1/|c_1|) \\ &\quad + c_2 = \tilde{\lambda}\sin^{-1}(\mp x_1/|c_1|) + c_2, \\ &m_{rr}(x_1(x_2), x_2, x_3) = \pm\tilde{\lambda}\sin^{-1}(x_2/|c_1|) \\ &\quad + c_3 = \tilde{\lambda}\sin^{-1}(\pm x_2/|c_1|) + c_3, \end{aligned} \tag{34}$$

where c_1, c_2 and c_3 are regarded as arbitrary constants of integration in the x_1x_2-plane, and, if necessary, may accordingly be considered as arbitrary functions of the third co-ordinate parameter, x_3.

The normal couple-stresses are then obtained by inserting either of (34b) and (34c) into (32). It is noted in this context, that specific values can be assigned to the appearing arbitrary constants only if appropriate boundary conditions are assigned on relevant boundaries of the polar material bar.

If, for instance, the following normal couple-traction boundary conditions are employed:

$$m_{11}|_{x_1=\pm L_1} = \hat{m}_1, \quad m_{22}|_{x_2=\pm L_2} = \hat{m}_2, \tag{35}$$

for given values of $\hat{m}_1$ and $\hat{m}_2$, then their combination with (32) and (34) reveals that

$$c_2 = \tilde{\lambda}\sin^{-1}(L_1/|c_1|) + \hat{m}_1/3,$$
$$c_3 = -\tilde{\lambda}\sin^{-1}(L_2/|c_1|) + \hat{m}_2/3, \tag{36}$$

and, hence, that two of the three arbitrary constants may be determined uniquely. It is thus noted that the choice $\hat{m}_1 = \hat{m}_2 = 0$ enables the lateral boundaries of the bar to be kept free from externally applied normal couple-stresses.

The outlined results imply that the considered polar transversely isotropic bar can maintain the deformed shape of its non-polar counterpart, depicted in Figure 1, only if the non-zero couple-stresses (31) are applied externally on their respective boundaries $x_\alpha = \pm L_\alpha$, along with (i) potentially nonzero normal couple-stresses, m_{11} and m_{22}, that may emerge on those boundaries, and (ii) the nonzero normal couple-stress distribution

$$m_{33}(x_1, x_2(x_1), 0) = -\tilde{\lambda}\left[\sin^{-1}|x_1/c_1| - \sin^{-1}(L_1/|c_1|)\right] + \hat{m}_1/3,$$
$$m_{33}(x_1(x_2), x_2, 0) = \tilde{\lambda}\left[\sin^{-1}|x_2/c_1| - \sin^{-1}(L_2/|c_1|)\right] + \hat{m}_2/3, \tag{37}$$

that will emerge on the boundary $x_3 = 0$.

However, $m_{33}(0,0,0)$ must attain a unique value at the bottom boundary of the bar, and a comparison of the pair of relevant values stemming from (37) reveals that the value of the last remaining constant, c_1, is defined as a root of the transcendental algebraic equation

$$\sin^{-1}(L_2/|c_1|) - \sin^{-1}(L_1/|c_1|) = (\hat{m}_1 + \hat{m}_2)/3\tilde{\lambda}. \tag{38}$$

The thus obtained value of c_1 then naturally feeds back into (36) and influences the value of the constants c_2 and c_3. Nevertheless, it also becomes understood that the lateral boundaries of the self-stretched polar material bar may be kept free from externally applied normal couple-stresses ($\hat{m}_1 = \hat{m}_2 = 0$) only if its cross-section on the x_1x_2-plane has the shape of a perfect square ($L_1 = L_2$).

After the couple-stress determination process thus is completed, (16b) is employed for the determination of the antisymmetric part of the stress tensor. It is accordingly observed that, since the right-hand side of (16b) depends on gradients of the couple-stress components, the emergent constant deviatoric couple-stresses (31) do not affect any of the stress components.

However, the fact that both (34b, c) depend on the in-plane coordinate parameters implies that, when combined with (32) and (16b), they give rise to four non-zero shear stress components, namely

$$\sigma_{32} = -\sigma_{23} = \sigma_{(32)} + \sigma_{[32]} = \frac{1}{6}m_{rr,1} = \frac{\tilde{\lambda}}{6x_2},$$
$$\sigma_{13} = -\sigma_{31} = \sigma_{(13)} + \sigma_{[13]} = \frac{1}{6}m_{rr,2} = -\frac{x_2}{6x_1}m_{rr,1} = -\frac{\tilde{\lambda}}{6x_1}, \tag{39}$$

where (2), (A.2) and (A.1) are also accounted for.

The appearance of these non-zero stress components implies that, for the polar material bar to maintain the deformed shape of its self-stretched non-polar counterpart, the tractions

$$\sigma_{13}\Big|_{x_1=\pm L_1} = \mp\frac{\tilde{\lambda}}{6L_1}, \quad \sigma_{23}\Big|_{x_2=\pm L_2} = \mp\frac{\tilde{\lambda}}{6L_2}, \sigma_{31}\Big|_{x_3=0,L} = \frac{\tilde{\lambda}}{6x_1},$$
$$\sigma_{32}\Big|_{x_3=0,L} = \frac{\tilde{\lambda}}{6x_2}, \tag{40}$$

must also be applied externally on its noted boundaries, in addition to the couple-traction boundary conditions stemming from (31) and (37).

The outlined results reveal that the displacement field (10) does not anymore represent the shape of a polar transversely isotropic bar deformed by its own weight. This is evidently because, like its non-polar material counterpart, a polar material bar stretched by its own weight is supposed to deform in the absence of any kind of externally applied tractions and couple-tractions.

As a matter of fact, a more critical look at the traction boundary conditions (40c) and (40d) further suggests that their exact implementation on the noted boundary is practically impossible. This is because either of those externally applied shear traction distributions is expected to attain a singular value at the co-ordinate origin ($x_1 = x_2 = 0$). Some potentially different solution of the PDE (33) may of course prevail and, thus, dismiss the observed singularity argument. However, even if such a solution does exist, and is found, it will not alter that principal relevant conclusion, according to which the deformation pattern of a polar fiber-reinforced bar differs from that of its non-polar polar material counterpart.

This conclusion is naturally anticipated also valid in the more general case of a specially orthotropic polar bar, where the relations (13) are dismissed and the general form of the constitutive equations (6) applies without simplifications. As will be seen later, in Section 5, the same is true even in the special case of polar material isotropy where, due to lack of fiber presence, polar material behavior is attributed to inherent, essentially unspecified, or even unknown properties of the material.

It necessarily follows that it is practically impossible for a polar material bar stretched by its own weight to attain, not only naturally but also artificially, the precise deformation pattern attained by its non-polar counterpart. While the problem of a self-stretched polar material bar thus remains still unsolved, and therefore open, Section 6 below discusses the manner that the results and new information reported in this communication will substantially assist ongoing developments regarding completion of its solution, as well as the solution of relevant boundary value problems in this subject.

4. Implication of the restricted versions of the theory

The preliminary concepts and equations detailed in Section 3.1 hold, essentially unaltered in the case of either of the two restricted versions of the full (unrestricted) theory considered in the preceding section. Each of those simpler versions of the theory applies some different type of restrictions into the part of the unrestricted theory that refers to polar material response only.

4.1. The fiber-splay deformation mode

The restricted, splay deformation version of the full theory arose in [7] during the search for an answer to an essentially curiosity driven question that emerges through strict adherence to and implementation in the strain energy function of the relationship

$$\kappa_{ij} = \kappa_{(ij)} + \kappa_{[ij]}. \tag{41}$$

This restriction leads to search for a special form of W^k that, unlike its unrestricted counterpart (22), obeys the symmetry condition

$$W^{\kappa}\big(\kappa_{(ij)}, \kappa_{[ij]}, a_i\big) = W^{\kappa}\big(\kappa_{[ij]}, \kappa_{(ij)}, a_i\big) = W^{\kappa}\big(\kappa_{ij}, a_i\big). \tag{42}$$

Application of this restriction necessarily leads to the simplified form

$$\begin{aligned} W^k &= \beta_1\big(\kappa_{(nn)}\big)^2 + \beta_2\kappa_{(nn)}a_k\kappa_{(km)}a_m + \hat{\beta}_3\big(a_k\kappa_{(km)}a_m\big)^2 \\ &= \beta_1\big(\kappa_{nn}\big)^2 + \beta_2\kappa_{nn}a_k\kappa_{km}a_m + \hat{\beta}_3\big(a_k\kappa_{km}a_m\big)^2, \end{aligned} \tag{43}$$

of the polar part of the strain energy function (22), and thus employs only three elastic moduli. Namely,

$$\beta_1 \geq 0, \ \ \beta_2 + \hat{\beta}_3 \geq 0, \ \ \hat{\beta}_3 \geq \beta_2^2/4\beta_1. \tag{44}$$

The constitutive equation (22) of the deviatoric couple-stress then also simplifies and becomes

$$\begin{aligned} \bar{m}_{\ell r} &= \frac{2}{3}\varepsilon_{r\ell s}a_s\big(2\beta_1\kappa_{nn} + \beta_2\kappa_{km}a_k a_m\big) \\ &= \frac{2}{3}\varepsilon_{r\ell s}a_s\big(2\beta_1\kappa_{(nn)} + \beta_2\kappa_{(km)}a_k a_m\big). \end{aligned} \tag{45}$$

It is seen that only two elastic moduli, β_1 and β_2, are thus left to actively participate into the this simplified constitutive equation. A third elastic modulus, $\hat{\beta}_3$, still regulates the extra energy term (25) that, although contributes into the strain energy part (43), leaves unaffected both the state of equilibrium and the constitutive equation (45)

In the present case of principal interest, where transverse isotropy is imposed through implementation of (26), this simplification leads to

$$\bar{m}_{\ell r} = \frac{2}{3}\varepsilon_{r\ell 3}\big(2\beta_1\kappa_{nn} + \beta_2\kappa_{33}\big). \tag{46}$$

which, in turn, enables replacement of the pair of non-zero deviatoric couple-stresses (31) with their marginally different counterparts

$$\bar{m}_{12} = -\bar{m}_{21} = -\rho g\hat{\lambda}, \ \ \hat{\lambda} = \frac{2}{3}[4\beta_1 S_{13} + (2\beta_1 + \beta_2)S_{33}]. \tag{47}$$

Apart from a replacement of the parameter λ defined in (31) (and appearing once more in (33)) with its slightly simplified counterpart $\hat{\lambda}$ defined in (47), the remaining of the analysis detailed in Section 3 remains completely unchanged. The remarkable similarity thus observed between the results stemming from the full version of the theory (Section 3) and its present restricted version is evidently due to the nature of the present polar elasticity problem, which is solely influenced by features of fiber-splay type deformations.

4.2. The fiber-bending deformation mode

The restricted, fiber-bending version of the theory employed in Section 3 makes use of the following curvature-strain part of the strain energy function [1, 4]:

$$W^K = \frac{3}{8}d^f K_j K_j + \bar{\gamma}\big(a_j K_j\big)^2, \ \ K_i = u_{i,kj}a_k a_j, \tag{48}$$

where K_i represents the fiber-curvature vector. This version makes use of only two additional elastic moduli, namely d^f and $\bar{\gamma}$, which are required to be non-negative. The observed simplification of (22) is then accompanied by a relevant simplification of the constitutive equation (30), which is replaced by the following:

$$\bar{m}_{\ell r} = \frac{4}{3}\varepsilon_{rsi}\frac{\partial W^K}{\partial K_i}a_\ell a_s. \tag{49}$$

In the present case of interest where (26) holds, (48) and (49) reduce to:

$$\begin{aligned} W^K &= \frac{3}{8}d^f K_j K_j + \bar{\gamma}K_3^2 = \frac{3}{8}d^f\big(K_1^2 + K_2^2 + K_3^2\big) + \bar{\gamma}K_3^2, \\ K_i &= u_{i,33}, \\ \bar{m}_{3r} &= \frac{4}{3}\varepsilon_{r3i}\frac{\partial W^K}{\partial K_i}. \end{aligned} \tag{50}$$

Nevertheless, by virtue of (10), (50b) yields

$$K_1 = K_2 = 0, \ \ K_3 = \rho g S_{33}, \tag{51}$$

and (50a) thus simplifies further, and becomes:

$$W^K = \left(\frac{3}{8}d^f + \bar{\gamma}\right)K_3^2 = \left(\frac{3}{8}d^f + \bar{\gamma}\right)(\rho g S_{33})^2. \tag{52}$$

It can then readily be verified, through combination of (50c) and (52), that the fiber-bending version of the theory predicts, inadequately, that (i) no deviatoric couple-stresses act on the bar and, hence, (ii) the polar part (52) is solely due to action of the spherical part of the couple stress; namely,

$$W^m = W^K = \left(\frac{3}{8}d^f + \bar{\gamma}\right)(\rho g S_{33})^2. \tag{53}$$

The latter result still enables formation of the PDE (33), with

$$\tilde{\lambda} = 6\rho g\left(\frac{3}{8}d^f + \bar{\gamma}\right)\frac{S_{33}^2}{S_{13}}, \quad (54)$$

and, henceforth, still endorses the spherical couple-stress analysis that leads to (37), (38) and (39). It, however, becomes understood that, due to absence or minimal fiber-bending deformation, the restricted fiber-bending version of the theory fails in this case to observe an important part of the polar material features captured earlier by the unrestricted theory.

It thus is fitting at this point to recall a very similar, essentially complementary observation made in Ref [8], in relation with the pure bending problem of a polar transversely isotropic plate. Since that polar elasticity problem is principally, if not exclusively influenced by features of fiber-bending type deformations, the restricted fiber-bending version produced marginally different results to those captured by the unrestricted theory. In contrast, due to lack of corresponding fiber-splay deformation features, it was the fiber-splay version of the theory that failed to reach any kind of reliable results and conclusions in that case.

5. Polar material isotropy

The special case of material isotropy is evidently characterized by complete absence of fibers or any other type of material preferential directions. The theory employed in section 3 thus becomes invalid in this case. However, by considering that the isotropic material of interest exhibits inherent polar material behavior, in the sense considered by Mindlin and Tiersten [19] and Koiter [16], the refined couple-stress theory presented in Ref [18] becomes valid instead.

5.1. Preliminary concepts

It is accordingly necessary in this case to initially employ the isotropic version of the non-polar constitutive equations (5) or (6), by noting that

$$S_{11} = S_{22} = S_{33} = 1/E, \;\; S_{12} = S_{13} = S_{23} = S_{23} = -\nu/E,$$

$$S_{44} = S_{55} = S_{44} = (1+\nu)/E, \quad (55)$$

where, as is already partially noted in (11), E and ν are the Young's modulus and the Poisson's ratio, respectively. It follows that the solution outlined earlier in Section 2, for the self-stretched fiber-reinforced bar, reduces now naturally to its isotropic counterpart presented in [15] and schematically represented in Figure 1.

In this case, the analysis detailed in Section 3.1 still holds, with the exception that (14) must be replaced with the following [3, 18]:

$$W = W^e(e_{ij}) + W^\Phi(\Phi_{i,j}) \geq 0, \quad (56)$$

where W^e is now the quadratic strain energy function of the non-polar isotropic solid and, in accordance with the refined version of the couple-stress theory [18],

$$W^\Phi(\Phi_{i,j}) = \frac{1}{2}m_{\ell i}\Phi_{i,\ell} = \frac{1}{2}\left(\frac{1}{3}m_{rr}\Phi_{\ell,\ell} + \bar{m}_{\ell i}\Phi_{i,\ell}\right), \quad (57)$$

is quadratic in the gradients of an auxiliary, virtual spin-vector $\mathbf{\Phi}$ (or, in components, Φ_i).

As is detailed in [3, 18], this virtual spin-vector is generally considered different from its actual, displacement generated counterpart $\mathbf{\Omega}$, defined and used in (18), but is still considered of the same order of magnitude with the displacement gradients. In this context, $\mathbf{\Phi}$ represents an infinite number of vectors that fulfill the single condition

$$W^\Phi(\Phi_{i,j}) = W^\Omega(\Omega_{i,j}) = \frac{1}{2}\bar{m}_{\ell i}\Omega_{i,\ell} \geq 0, \quad (58)$$

and, for this reason, it does not need to ultimately be determined.

Nevertheless, satisfaction of the condition (58) suffices to guarantee validity of the PDE (18a) that enables determination of m_{rr} and, henceforth, of the spherical part of the couple-stress (e.g. [3, 18]). It is emphasized in this context that the definition (57) implies that W^Φ does account for the contribution of the spherical part of the couple-stress. In contrast, (58) reveals that W^Ω does not do so, due to the implication of the mathematical identity (18c).

In other words, the last part of (58) implies that the special case of the conventional couple-stress ($\mathbf{\Phi} = \mathbf{\Omega}$) emerges as a singular case in which the spherical part of the couple-stress is not accounted for. It is also noted that, along with (58), the outlined observations hold true for isotropic as well as for anisotropic polar materials, including fiber-reinforced materials with fiber-bending stiffness [2, 3, 18, 20].

5.2. Constitutive equations

While the constitutive equation (15b) that provides the symmetric part of the stress still holds, its polar part (20) is now replaced by the following [3, 18]:

$$m_{ji} = \frac{\partial W^\Phi}{\partial \Phi_{i,j}}. \quad (59)$$

In accordance with the symmetries of material isotropy, the polar part of the strain energy function (56) attains the form [18]

$$W^\Phi(\Phi_{m,n}) = \frac{1}{2}\left[\eta_0(\Phi_{m,m})^2 + \eta_1\Phi_{(m,n)}\Phi_{(n,m)} + \eta_2\Phi_{[m,n]}\Phi_{[n,m]}\right], \quad (60)$$

where

$$\Phi_{(i,j)} = \frac{1}{2}(\Phi_{i,j} + \Phi_{j,i}), \;\; \Phi_{[i,j]} = \frac{1}{2}(\Phi_{i,j} - \Phi_{j,i}), \quad (61)$$

represent the symmetric and antisymmetric parts of $\Phi_{i,j}$, respectively. Moreover, the appearing material moduli η_0, η_1

and η_2 are all considered non-negative, so that the positive semi-definiteness conditions (58) are satisfied.

A combination of (59) and (60) then provides the couple-stress constitutive equation in the following form:

$$m_{ji} = \frac{\partial W^{\Phi}}{\partial \Phi_{i,j}} = \eta_0 \Phi_{m,m}\delta_{ij} + 2\eta_1 \Phi_{(i,j)} + 2\eta_2 \Phi_{[j,i]}$$
$$= \eta_0 \Phi_{m,m}\delta_{ij} + (\eta_1+\eta_2)\Phi_{j,i} + (\eta_1-\eta_2)\Phi_{i,j}, \tag{62}$$

which, through contraction of the appearing free indices, yields

$$m_{rr} = \frac{\partial W^{\Phi}}{\partial \Phi_{r,r}} = (3\eta_0 + 2\eta_1)\Phi_{r,r}. \tag{63}$$

In the singular case of the conventional couple-stress theory [16, 19], where $\mathbf{\Phi}$ is chosen to coincide with $\mathbf{\Omega}$, the identity (18c) invalidates (62) while, at the same time, forces (60) to attain the form

$$W^{\Omega}(\Omega_{m,n}) = \frac{1}{2}\left[\eta_1 \Omega_{(m,n)}\Omega_{(n,m)} + \eta_2 \Omega_{[m,n]}\Omega_{[n,m]}\right]. \tag{64}$$

As is detailed in [18], it thus becomes necessary for the constitutive equation (62) to be replaced by its conventional theory counterpart [16, 19],

$$\bar{m}_{ji} = \frac{\partial W^{\Omega}}{\partial \Omega_{i,j}} = 2\eta_1 \Omega_{(i,j)} + 2\eta_2 \Omega_{[j,i]}$$
$$= (\eta_1+\eta_2)\Omega_{j,i} + (\eta_1-\eta_2)\Omega_{i,j}. \tag{65}$$

When combined with the condition (58), these considerations make it evident that full development of the PDE (18a) is achieved by associating to it the extra energy term

$$W^m = \eta_0 (\Phi_{m,m})^2/2, \tag{66}$$

thus leading to

$$\Omega_\ell m_{rr,\ell} = 3\eta_0 (\Phi_{m,m})^2 - 3(\bar{m}_{\ell i}\Omega_i)_{,\ell}. \tag{67}$$

Hence, a combination of this equation with (63) yields

$$\Omega_\ell m_{rr,\ell} = \eta m_{rr}^2 - 3(\bar{m}_{\ell i}\Omega_i)_{,\ell}, \quad \eta = \frac{3\eta_0}{(3\eta_0+2\eta_1)^2} > 0, \tag{68}$$

which is a non-linear PDE for the unknown spherical part of the couple-stress, m_{rr}.

5.3. Effect of polar material behavior on the solution of the non-polar elasticity problem

In the present case of interest, where (55) holds, the components (19) of the actual spin vector become

$$\Omega_1 = \frac{\rho g \nu}{E} x_2, \quad \Omega_2 = -\frac{\rho g \nu}{E} x_1, \quad \Omega_3 = 0. \tag{69}$$

The only nonzero components of the deviatoric couple-stress tensor (65), namely

$$\bar{m}_{12} = -\bar{m}_{21} = \rho g \frac{2\eta_2 \nu}{E}, \tag{70}$$

thus remain constant and opposite.

The deviatoric normal couple-stresses are then still all zero ($\bar{m}_{11} = \bar{m}_{22} = \bar{m}_{33} = 0$) and, as a result, (17) still returns

$$m_{11} = m_{22} = m_{33} = \frac{1}{3} m_{rr}. \tag{71}$$

It follows that determination of the normal couple-stress components requires solution of the PDE

$$x_1 m_{rr,2} - x_2 m_{rr,1} + \bar{\eta} m_{rr}^2 = -\bar{\lambda},$$
$$\bar{\eta} = \frac{3\eta_0 E}{(3\eta_0+2\eta_1)^2 \rho g \nu}, \quad \bar{\lambda} = 12\eta_2 \frac{\rho g \nu}{E}, \tag{72}$$

which is obtained by inserting (69) and (70) into (68).

Exhaustive search for potential solutions of this non-linear PDE is beyond the purpose of this investigation. However, it is initially observed that, regardless of the sign of the Poisson ratio ($-1 \leq \nu \leq 1/2$), the constants $\bar{\eta}$ and $\bar{\lambda}$ are of the same sign. It follows that, unlike its counterpart met and solved in Section 5.2 of [18], the PDE (72) does not admit real constant solutions for m_{rr}.

Nevertheless, at least one variable solution of the PDE (72) can be found with use of the method of characteristics. As is briefly outlined in Appendix A, this may be described as follows:

$$x_1^2 + x_2^2 = c_1^2,$$
$$m_{rr} = \sqrt{\bar{\lambda}/\bar{\eta}} \tan\left\{\sqrt{\bar{\lambda}\bar{\eta}} \sin^{-1}(\pm x_1/|c_1|) + c_2\right\}, \tag{73}$$
$$m_{rr} = \sqrt{\bar{\lambda}/\bar{\eta}} \tan\left\{\sqrt{\bar{\lambda}\bar{\eta}} \sin^{-1}(\mp x_2/|c_1|) + c_3\right\},$$

where c_1, c_2 and c_3 are again regarded as arbitrary constants of integration in the x_1x_2-plane. The normal couple-stresses are then still obtained by inserting either of (73b, c) into (71).

Unique determination of the appearing arbitrary constants may be achieved with introduction and use of some appropriate relevant set of normal couple-stress boundary conditions, in a manner analogous to that described earlier in Section 3.3, regarding the solution (34) of the PDE (33). The corresponding analysis will thus not be repeated or pursued any further. However, the expectation has already been confirmed that, naturally, the deformation pattern of an isotropic polar material bar stretched by its own weight differs to that of its non-polar material counterpart.

6. Further discussion and conclusions

The fact that activation of "internal moment-tractions" prevents a heterogeneous composite from maintaining the deformation pattern of its corresponding homogeneous counterpart is not surprising. This is, for instance, a well-known response feature of functionally graded composites (e.g. [13–14] and references therein). In this regard, even manufacturing imperfections can claimed as sources of couple-stress action that affects the deformation pattern of macroscopically homogeneous anisotropic structural components.

In the special case of piece-wise functional gradation (thin-walled layered composites) that response feature of composites was arguably first modeled and captured, as early as 1961 [21], with use of non-polar symmetric elasticity tools. Namely, with a combination of non-polar (symmetric-) elasticity principles and the widely known and employed method of two-dimensional, smeared plate modeling. That remarkable publication [21] appeared during a period that emergence of the conventional couple-stress theory [16, 19, 22] revitalized interest in the Cosserat theory [23] and, thus, initiated the ongoing extension of three-dimensional elasticity that captures effects of polar material behavior.

It thus is not surprising either, that, unless specific, extra traction and/or couple-traction distributions are appropriately imposed on the external boundaries of a polar material structure, its deformed configuration will differ from that observed when its non-polar material counterpart is subjected to identical loading conditions. The specific problem of a polar material prismatic bar/plate stretched by its own weight considered in this study, along with the pure bending problem of a polar material plate (e.g. [6, 8, 16]), are among the simplest relevant examples that comply with this observation.

As far as the subject of the present communication is concerned, these considerations imply that the actual deformation pattern attained by a self-stretched polar material bar is still not known. Nevertheless, the same is essentially true for the deformation pattern attained by a polar material plate subjected to standard, simple bending loading conditions only; namely, boundary conditions that are deprived assistance from extra boundary couple-tractions, such as those imposed in [4–6, 8]. In this regard, the polar material version of either of these fundamental elasticity problems remains, at least partially, unsolved and, therefore, open to further investigation and study.

These observations are consistent with the feeling that couple-stresses are usually generated during the deformation of a polar material structure by internal and/or inherent material properties and features, rather than through externally applied couple-traction boundary conditions. This is normally the rule rather than an exception. Hence, given the difficulties that one may meet in attempting to solve the governing differential equations of polar material elasticity, energy minimization techniques naturally emerge as a potential source of relevant, additional mathematical tools.

In this context, attention is next directed into relevant benefits that may become available through suitable use of the following:

"*Theorem of minimum potential energy in generally anisotropic polar linear elasticity*

Of all continuous displacement fields $\boldsymbol{u}^*$ which (i) satisfy the displacement related boundary conditions on the relevant part, S^u, of the bounding surface S, and (ii) possess up to third-order continuous and differentiable derivatives, the field $\boldsymbol{u}$ that represents the single continuous solution of a well-posed boundary value problem in polar linear elasticity yields a minimum value of the potential energy functional

$$P(u_i) = \int_V \left[W^e(e_{ij}) + 2W^\omega(\omega_{ij})\right]dV - \int_{S^T} T_i^B u_i dS - \int_V F_i u_i dV, \tag{74a}$$

or, equivalently,

$$P(u_i) = \int_V \left[W^e(e_{ij}) + 2W^\Omega(\Omega_{i,j})\right]dV - \int_{S^T} \left(T_i^B u_i + L_i^B \Omega_i\right)dS - \int_V F_i u_i dV, \tag{74b}$$

where V is the volume surrounded by S $(= S^u \cup S^T)$, S^T represents the part of S that boundary tractions, T_i^B, and boundary couple-tractions, L_i^B, are prescribed on and F_i is the vector of the body forces."

In close relevance with the standard definition of non-polar material part of the strain energy function, namely (15a), the rotation and spin energies appearing in (74a, b) are respectively defined according to

$$W^\omega(\omega_{ij}) = \frac{1}{2}\sigma_{[ji]}\omega_{ij}, \quad W^\Omega(\Omega_{i,j}) = \frac{1}{2}m_{\ell i}\Omega_{i,\ell} = \frac{1}{2}\bar{m}_{\ell i}\Omega_{i,\ell}, \tag{75}$$

where (17) and (18c) are also accounted for (see also [16, 19]). These energy quantities have been shown related as follows [6]:

$$W^\omega(\omega_{ij}) = W^\Omega(\Omega_{i,j}) - \frac{1}{2}\left(m_{ij}\Omega_j\right)_{,i}. \tag{76}$$

Hence, (75b) implies that W^Ω is directly relevant to the action of the deviatoric couple-stress only, while a combination of (76) and (17) reveals that the spherical part of the couple-stress is involved in the W^ω definition and formation as well.

Moreover, Cauchy's formula gives the components of the traction and the couple-traction vectors acting on any internal or bounding surface of the material, as follows:

$$T_i^{(n)} = \sigma_{ji}n_j, \qquad L_i^{(n)} = m_{ji}n_j, \tag{77}$$

where $\boldsymbol{n}$ denotes the outward unit normal of that surface. It thus is recalled that these formulas are also naturally consistent with the boundary traction vectors, T_i^B and L_i^B, appearing in (74).

In the absence of body forces, a proof of the afore mentioned polar material version of the theorem of minimum potential energy can be found in [6]. Nevertheless, a slightly enhanced version of that proof is also presented in Appendix B, for self-sufficiency of this study.

A modified version of the theorem that becomes available by virtue of (58) enables replacement of W^Ω with W^Φ in (74b). The theorem then is seen also valid after replacement of the actual spin vector, $\boldsymbol{\Omega}$, by its virtual counterpart, $\boldsymbol{\Phi}$, provided that the latter is also required to satisfy the additional condition:

$$\int_{S^T} L_i^B(\Omega_i - \Phi_i)dS = 0. \tag{78}$$

It is noted that, in that case, the pair of conditions (58) and (78) is still insufficient for unique determination of all three components of Φ_i, which thus remains a virtual spin vector.

Such a modified version of the theorem may be found useful in cases that $\mathbf{\Phi}$ can somehow be specified in advance and, thus, replace $\mathbf{\Omega}$ in its role as actual spin vector (e.g. [8]). However, as is also shown in recent relevant studies [2, 3, 18, 20] precise determination of the vector $\mathbf{\Phi}$ is unnecessary. Hence, the present version of the theorem is adequate for the purposes of this study, at least as far as solution to problems related with isotropic polar elasticity is concerned (e.g. Section 5).

Nevertheless, and regardless of potential implementation of (78), the following extension of the condition (58):

$$W^k(\boldsymbol{\kappa}) = W^{\Phi}\left(\Phi_{i,j}\right) = W^{\Omega}\left(\Omega_{i,j}\right) = \frac{1}{2}\bar{m}_{\ell i}\Omega_{i,\ell} \geq 0, \qquad (79)$$

enables connection to be established between the fiber-stiffness generated polar material behavior implied in (14) and the action of some auxiliary spin vector, $\mathbf{\Phi}$. Although (79) is still insufficient for unique determination of that vector, it suffices to guarantee validity of the PDE (18a) that leads to determination of the spherical part of the couple-stress.

In this context, the afore mentioned theorem of minimum potential energy is also seen adequate in looking for solution to problems related with polar material behavior of linearly elastic fiber-reinforced materials with fiber-bending stiffness. It is worth mentioning that this extension of the theorem's applicability refers not only to the relevant unrestricted theory that makes use of eight fiber-bending elastic moduli (Section 3), but also to its restricted fiber-splay (Section 4.1) and fiber-bending (Section 4.2) deformation versions, which make use of only three and two such moduli, respectively.

It is further worth noting that integration of (76) over an arbitrary volume V, surrounded by a closed surface S of the solid, leads to

$$\int_V \left[W^{\Omega}\left(\Omega_{i,j}\right) - W^{\omega}\left(\omega_{ij}\right)\right]dV = \frac{1}{2}\int_S L_i^{(n)}\Omega_i dS, \qquad (80)$$

where use is made of the divergence theorem as well as (77b). Hence, in the special case that, as happens in (74), V represents the total volume of the solid, (80) yields:

$$\int_V \left[W^{\Omega}\left(\Omega_{i,j}\right) - W^{\omega}\left(\omega_{ij}\right)\right]dV = \frac{1}{2}\int_{S^T} L_i^B\Omega_i dS. \qquad (81)$$

This result thus clarifies the source of the equivalence noted between (74a) and (74b).

Moreover, (81) reveals that the difference of the total amount of energies produced by the local energy quantities W^{Ω} and W^{ω} equals one half of the work done by the boundary couple-tractions. As a matter of fact, although W^{Ω} and W^{ω} represent different amounts of energy locally, their total amounts are evidently equal in the absence of boundary couple-tractions ($L_i^B = 0$). Indeed, the total amounts of W^{Ω} and W^{ω} are different only when boundary couple-tractions are present ($L_i^B \neq 0$).

The outlined discussion makes it clear that, regardless of the presence or absence of boundary couple-tractions, minimization of either form of the potential energy functional (74) can lead to full determination of the solution of any relevant boundary value problem; including, of course, the problem of a self-stretched polar material bar. However, polar material response requires from (74a) and (74b) to be treated in a different manner.

In more detail, since the functional (74b) makes no use of the spherical part of the couple-stress, its minimization will naturally lead to determination of the displacement, the symmetric stress and the deviatoric couple-stress fields only. Determination of the spherical part of the couple-stress and, henceforth, of the antisymmetric part of, and the full stress field can then be pursued by solving the corresponding PDE stemming from (18a), through use of some suitable analytical or numerical/computational method.

In contrast, the fact that the (74a) does make use of m_{rr} implies that, in this alternative form, the potential energy functional cannot be minimized independently of the PDE (18a). With that PDE thus acquiring the role of a constraint during such a minimization process, the form (74a) of the potential energy functional must be modified and obtain the form:

$$P(u_i) = \int_V \Big\{ W^e(e_{ij}) + 2W^{\omega}(\omega_{ij}) + \Lambda[\Omega_{\ell} m_{rr,\ell} - 6W^m$$

$$+3(\bar{m}_{\ell i}\Omega_i)_{,\ell}]\Big\}dV - \int_{S^T} T_i^B u_i dS - \int_V F_i u_i dV, \qquad (82)$$

where the appearing additional unknown, Λ, represents a standard Lagrange multiplier.

Either in this pair of equivalent processes of potential energy minimization may practically be found superior (or more economical) to its alternative. However, no clear relevant evidence is available at present.

Disclosure statement

No potential conflict of interest was reported by the author(s).

References

[1] A.J.M. Spencer, and K.P. Soldatos, Finite deformations of fibre-reinforced elastic solids with fibre bending stiffness, Int. J. Non-Lin. Mech., vol. 42, no. 2, pp. 355–368, 2007. DOI: 10.1016/j.ijnonlinmec.2007.02.015.

[2] K.P. Soldatos, Finite deformations of fibre-reinforced elastic solids with fibre bending stiffness – Part II: determination of the spherical part of the couple-stress, Math. Mech. Solids., vol. 28, no. 1, pp. 124–140, 2023.). DOI: 10.1177/10812865211061595.

[3] K.P. Soldatos, New trends in couple-stress hyperelasticity, Math. Mech. Solids., pp. 108128652311776, 2023. DOI: 10.1177/10812865231177673).

[4] K.P. Soldatos, Foundation of polar linear elasticity for fibre-reinforced materials, J. Elast., vol. 114, no. 2, pp. 155–178, 2014. DOI: 10.1007/s10659-013-9433-6.

[5] K.P. Soldatos, On the characterisation of fibrous composites when fibres resist bending, Int. J. Solids Struct., vol. 148-149, pp. 35–43, 2018.). DOI: 10.1016/j.ijsolstr.2017.10.001.

[6] K.P. Soldatos, On the characterisation of fibrous composites when fibres resist bending - Part II: connection with anisotropic polar linear elasticity, Int. J. Solids Struct., vol. 152-153, pp. 1–11, 2018. DOI: 10.1016/j.ijsolstr.2018.08.022).

[7] K.P. Soldatos, M.H.B.M. Shariff, and J. Merodio, On the constitution of polar fibre-reinforced materials, Mech. Adv. Mater. Struct., vol. 28, no. 21, pp. 2255–2266, 2021. DOI: 10.1080/15376494.2020.1729449.
[8] K.P. Soldatos, Determination of the spherical part of the couple-stress in a polar fibre-reinforced elastic plate subjected to pure bending, Acta Mech., vol. 232, no. 10, pp. 3881–3896, 2021.). DOI: 10.1007/s00707-021-03035-z.
[9] M.A. Dagher, and K.P. Soldatos, Pure azimuthal shear deformation of an incompressible tube reinforced by radial fibres resistant in bending IMA, J. Appl. Math., vol. 79, no. 5, pp. 848–868, 2014. DOI: 10.1093/imamat/hxu013).
[10] M.A. Dagher, and K.P. Soldatos, Area-preserving azimuthal shear deformation of an incompressible tube reinforced by radial fibres, J. Eng. Math., vol. 95, no. 1, pp. 101–119, 2015. DOI: 10.1007/s10665-014-9728-z).
[11] A.F. Farhat, and K.P. Soldatos, Cylindrical bending and vibration of polar material laminates, Mech. Adv. Mater. Struct., vol. 22, no. 11, pp. 885–896, 2015. DOI: 10.1080/15376494.2013.864438.
[12] K.P. Soldatos, and A.F. Farhat, On Reissner's displacement field in modelling thin elastic plates with embedded fibres resistant in bending, IMA J. Appl. Math., vol. 81, no. 6, pp. 1076–1095, 2016. DOI: 10.1093/imamat/hxw045.
[13] K.P. Soldatos, M. Aydogdu, and U. Gul, Plane strain polar elasticity of fibre reinforced functionally graded materials and structures, J. Mech. Mater. Struct., vol. 14, no. 4, pp. 497–535, 2019. DOI: 10.2140/jomms.2019.14.497.
[14] M. Aydogdu, T. Aksencer, and K.P. Soldatos, On three-dimensional dynamics of fibre-reinforced functionally graded plates when fibres resist bending, J. Eng. Math., vol. 128, no. 1, pp. 13, 2021. DOI: 10.1007/s10665-021-10128-0.
[15] S.P. Timoshenko, and J.N. Goodier, 1970. Theory of Elasticity, 3rd ed. McGraw Hill, New York.
[16] W.T. Koiter, Couple stresses in the theory of elasticity, I and II, Proc. Ned. Akad. Wet. Ser B., vol. 67, pp. 17–44, 1964.
[17] R.M. Jones, 1998. Mechanics of Composite Materials. Taylor & Francis, Washington.
[18] K.P. Soldatos, Determination of the spherical couple-stress in polar linear isotropic elasticity, J. Elast., vol. 153, no. 2, pp. 185–206, 2023. DOI: 10.1007/s10659-022-09979-0).
[19] R.D. Mindlin, and H.F. Tiersten, Effects of couple-stresses in linear elasticity, Arch. Rational Mech. Anal., vol. 11, no. 1, pp. 415–448, 1962. DOI: 10.1007/BF00253946.
[20] K.P. Soldatos, Refined anisotropic couple-stress elasticity, Math. Mech. Solids, 2024. DOI: 10.1177/10812865231222898.
[21] E. Reissner, and Y. Stavsky, Bending and stretching of certain types of heterogeneous aeolotropic plates, ASME J. Appl. Mech., vol. 28, no. 3, pp. 402–408, 1961. DOI: 10.1115/1.3641719.
[22] C. Truesdell, and R.A. Toupin, 1960. The classical field theories. Encycl. Phys, vol. III, no. 1, 226–793 Springer-Verlag, Berlin.
[23] E. Cosserat, and F. Cosserat, 1909. Théorie des Corps Deformables. Hermann, Paris.

Appendix A: Solution of the PDEs (33) and (72) with the method of characteristic lines

Application of the method of characteristics on the PDE (33) requires a search for plane curves (on the x_1x_2-plane) whose tangent satisfies the ordinary differential equation (ODE)

$$\frac{dx_2}{dx_1} = -\frac{x_1}{x_2}. \tag{A.1}$$

Integration of this equation reveals that the characteristic lines sought are the circles (34a), where the otherwise arbitrary constant of integration, c_1^2, is necessarily selected positive.

By virtue of (A.1), the PDE (33) can next be transformed into either of the ODEs

$$\frac{dm_{rr}}{dx_1} = -\frac{\tilde{\lambda}}{x_2} = \mp\frac{\tilde{\lambda}}{|c_1|\sqrt{1-x_1^2/c_1^2}}, \quad \frac{dm_{rr}}{dx_2} = \frac{\tilde{\lambda}}{x_1} = \pm\frac{\tilde{\lambda}}{|c_1|\sqrt{1-x_2^2/c_1^2}} \tag{A.2}$$

where use is also made of (34a). The solution sought of the PDE (33) is completed by integrating the ODEs (A.2a) and (A.2b), thus, respectively leading to (34b) and (34c) that involve two additional arbitrary constants of integration, c_2 and c_3.

In a similar manner, solution of the PDE (72) departs again with integration the ODE (A.1) and, thus, that leads again to the circular characteristic lines (34a); also quoted in (73a). Validity of (A.1) then enables transformation of (72) into either of the following ODEs

$$\frac{dm_{rr}}{m_{rr}^2+\bar{\lambda}/\bar{\eta}} = \bar{\eta}\frac{dx_1}{x_2} = \pm\bar{\eta}\frac{dx_1}{|c_1|\sqrt{1-x_1^2/c_1^2}}, \quad \frac{dm_{rr}}{m_{rr}^2+\bar{\lambda}/\bar{\eta}} = -\bar{\eta}\frac{dx_2}{x_1} = \mp\bar{\eta}\frac{dx_1}{|c_1|\sqrt{1-x_2^2/c_1^2}}. \tag{A.3}$$

Direct integration of these equations yields

$$\begin{aligned} \tan^{-1}\left(m_{rr}/\sqrt{\bar{\lambda}/\bar{\eta}}\right) &= \bar{\eta}\sqrt{\bar{\lambda}/\bar{\eta}}\sin^{-1}(\pm x_1/|c_1|)+c_2, \\ \tan^{-1}\left(m_{rr}/\sqrt{\bar{\lambda}/\bar{\eta}}\right) &= \bar{\eta}\sqrt{\bar{\lambda}/\bar{\eta}}\sin^{-1}(\mp x_2/|c_1|)+c_3, \end{aligned} \tag{A.4}$$

and thus leads to a solution of (72) that is described in (73).

Appendix B: Proof of the theorem of minimum potential energy in couple-stress elasticity

The standard form that of the equilibrium equation is

$$\sigma_{ji,j} + F_i = 0, \tag{B.1}$$

where, **F** represents the body force vector. It is recalled, for completeness, that its alternative form (16a) attained earlier in Section 3 is obtained after the appearing stress tensor splits into its symmetric and antisymmetric parts, and further use is also made of (16b).

Multiplying both sides of (B.1) by the vector $\boldsymbol{u} - \boldsymbol{u}^*$ and then integrating over the volume V of the elastic body, one obtains

$$\int_V (\sigma_{ji,j}+F_i)(u_i-u_i^*)dV = 0, \tag{B.2}$$

or, equivalently,

$$\int_V \left\{ \left[\sigma_{ji}(u_i-u_i^*)\right]_{,j} - \sigma_{ji}\left(u_{i,j}-u_{i,j}^*\right) + F_i(u_i-u_i^*)\right\}dV = 0. \tag{B.3}$$

Applying the divergence theorem on the first term of the integrant and, also, splitting all tensorial quantities appearing in the second term into their symmetric and anti-symmetric parts, one obtains

$$\int_S n_j\sigma_{ji}(u_i-u_i^*)dS + \int_V F_i(u_i-u_i^*)dV = \int_V \left[\sigma_{(ji)}\left(e_{ij}-e_{ij}^*\right) + \sigma_{[ji]}\left(\omega_{ij}-\omega_{ij}^*\right)\right]dV, \tag{B.4}$$

where the definitions (7) are accounted for, and quantities marked with an asterisk relate to $\boldsymbol{u}^*$ in the same manner that their unmarked counterparts relate to $\boldsymbol{u}$.

By virtue of (77a), (15) and (16b), one next obtains

$$\int_S T_i^{(n)}(u_i-u_i^*)dS + \int_V F_i(u_i-u_i^*)dV = \int_V \left\{ c_{ijk\ell}e_{k\ell}\left(e_{ij}-e_{ij}^*\right) - \frac{1}{2}\varepsilon_{kji}m_{\ell k,\ell}\left(\omega_{ij}-\omega_{ij}^*\right)\right\}dV, \tag{B.5}$$

where $\mathbf{c}$ is the fourth-order tensor of elastic moduli met in non-polar, symmetric-stress linear elasticity. In this regard, it is fitting at this point to also note the following identity:

$$c_{ijk\ell}e_{k\ell}\left(e_{ij}-e_{ij}^{*}\right)=\frac{1}{2}c_{ijk\ell}\left[e_{k\ell}e_{ij}+\left(e_{k\ell}-e_{kl}^{*}\right)\left(e_{ij}-e_{ij}^{*}\right)-e_{kl}^{*}e_{ij}^{*}\right]$$
$$=W^{e}(e_{ij})+W^{e}\left(e_{ij}-e_{ij}^{*}\right)-W^{e}\left(e_{ij}^{*}\right), \tag{B.6}$$

whose validity stems from the standard symmetries,

$$c_{ijk\ell}=c_{jik\ell}=c_{k\ell ij}, \tag{B.7}$$

obeyed by the components of the elastic moduli tensor, $\mathbf{c}$.

By appropriately using the product rule of differentiation and the divergence theorem on the last term of its right-hand side, (B.5) then leads to

$$\int_S T_i^{(n)}(u_i-u_i^*)dS+\int_V F_i(u_i-u_i^*)dV=\int_V c_{ijk\ell}e_{k\ell}\left(e_{ij}-e_{ij}^*\right)dV- \left\{\int_S m_{\ell k}\left(\Omega_k-\Omega_k^*\right)n_\ell dS-\int_V \bar{m}_{\ell k}\left(\Omega_{k,\ell}-\Omega_{k,\ell}^*\right)dV\right\}, \tag{B.8}$$

where validity of (18b, c) and (17) enabled implementation of the following intermediate results:

$$\frac{1}{2}\varepsilon_{kji}m_{\ell k}\left(\omega_{ij}-\omega_{ij}^{*}\right)=m_{\ell k}\left(\Omega_k-\Omega_k^*\right),$$
$$\frac{1}{2}\varepsilon_{kji}m_{\ell k}\left(\omega_{ij}-\omega_{ij}^{*}\right)_{,\ell}=m_{\ell k}\left(\Omega_k-\Omega_k^*\right)_{,\ell}=\left(\bar{m}_{\ell k}+\frac{1}{3}m_{rr}\delta_{\ell k}\right)$$
$$\left(\Omega_{k,\ell}-\Omega_{k,\ell}^*\right)=\bar{m}_{\ell k}\left(\Omega_{k,\ell}-\Omega_{k,\ell}^*\right). \tag{B.9}$$

Use of (77b) and (75b), as well as of the fact $\boldsymbol{u}-\boldsymbol{u}^*=\boldsymbol{\Omega}-\boldsymbol{\Omega}^*=0$ on S^u, enables (B.8) to transform into:

$$\int_{S^T} T_i^B(u_i-u_i^*)dS+\int_V F_i(u_i-u_i^*)dV=\int_V c_{ijk\ell}e_{k\ell}\left(e_{ij}-e_{ij}^*\right)dV- \int_S L_k^{(n)}\left(\Omega_k-\Omega_k^*\right)dS+2\int_V\left[W^{\Omega}\left(\Omega_{i,j}\right)-W^{\Omega}\left(\Omega_{i,j}^*\right)\right]dV, \tag{B.10}$$

or, through use of (78), into the equivalent form:

$$\int_{S^T} T_i^B\left(u_i-u_i^*\right)dS+\int_V F_i\left(u_i-u_i^*\right)dV=\int_V c_{ijk\ell}e_{k\ell}\left(e_{ij}-e_{ij}^*\right)dV +2\int_V\left[W^{\omega}(\omega_{ij})-W^{\omega}\left(\omega_{ij}^*\right)\right]dV. \tag{B.11}$$

Hence, upon applying the identity (B.6) in the first integral appearing on the right-hand side, and then appropriately rearranging the terms of the resulting equation with the help of the definition (74a), one obtains:

$$P\left(u_i^*\right)-P(u_i)=W^{e}\left(e_{ij}-e_{ij}^*\right)\geq 0, \tag{B.12}$$

which proves the theorem. It may be noted that, due to the positive definiteness of W^e, equality holds only when $\boldsymbol{u}$ and $\boldsymbol{u}^*$ produce identical continuous strain fields ($\boldsymbol{e}=\boldsymbol{e}^*$).

Finally, the equivalence of the potential energy definitions (74a) and (74b) is essentially implicit in (B.10). This becomes evident by noting that, like its left-hand side counterpart, the surface integral appearing in the right-hand side of (B.10) is essentially confined over the S^T part of the bounding surface, where the traction vectors $L_k^{(n)}$ and L_k^B are necessarily equal. Hence, use of the identity (B.9) on the right-hand side of (B.10), followed by term rearrangement that is guided by (74b), yields again (B.12).